CHEMICAL ENGINEERING TRANSACTIONS
VOL. 43, 2015
A publication of AIDIC
The Italian Association of Chemical Engineering
Online at www.aidic.it/cet
Chief Editors: Sauro Pierucci, Jiří J. Klemeš

**ISBN** 978-88-95608-34-1; **ISSN** 2283-9216
DOI: 10.3303/CET1543282

# Obtaining the Nusselt Equation with the Use of CFD for a Stirred Tank Heated with Helical Coils

Ronald Jaimes, Jose R. Nunhez*

School of Chemical Engineering, University of Campinas – UNICAMP, Albert Einstein avenue 500, CEP: 13083-970, Campinas, Brazil
nunhez@feq.unicamp.br

Stirred Tank Reactors (STR) are widely used in the chemical industry. When these tanks are used for highly exothermic reactions, a jacket or coils are employed for heat removal. Inner coils are used to supply additional heat transfer surfaces in stirred tanks when the needed heat generation or removal is too great. One major problem associated with inner coils is that they provide resistance or blockage to flow, reducing the effective flow circulation within the reactor. The aim of this work is to obtain a CFD model for these systems in order to improve their design. In the first part of the work a methodology is proposed to obtain a CFD Nusselt correlation according to the work by Oldshue and Gretton (1954). After this step, the design proposed by Pedrosa and Nunhez (2003) will be simulated and compared to the geometry by Oldshue and Gretton (1954). Preliminary results indicate that the CFD model reproduces the correlation by Oldshue and Gretton (1954).

## 1. Introduction

The operations of crystallization, liquid-liquid extraction, leaching, heterogeneous catalytic reactions, and fermentation are some examples of industrial operations carried out in Stirred Tank Reactors. The main purpose of these devices is to achieve product homogenization, uniform heat and mass transfer (Paul et al., 2004). To ensure homogenization, one or more impellers are used to generate desired flow and mixing within these devices. In reactions where the heat of reaction is high, the heating or cooling of the reaction system is necessary to increase the efficiency of the reaction (equilibrium of reaction) and ensure safe operation. To keep the fluid in the reactor at the desired temperature, heat must be added or removed by a jacket on the tank wall and/or through coils (axial or helical) immersed in the fluid with aims of promoting heat transfer. Experimental studies have the advantage of dealing with the real configuration. However, physical experiments can be expensive and time consuming. Furthermore, full-scale experimentation can often not be performed for large systems or systems involving dangerous materials. Computational Fluid Dynamics (CFD) is an alternative technique that can be used to reduce cost and provide support in scale-up process. In general, CFD provides a deeper understanding of the processes of fluid flow, making experimental research more efficient.

## 2. Methodology

Below will be described the technique employed for the numerical simulation and analysis of the influence of the position of the coils of a stirred tank reactor with respect to the fluid flow and temperature distribution in the turbulent regime. The physical phenomenon involved in the movement of fluid in the stirring and mixing process was modelled using the equations of conservation of mass, momentum, and energy. The equations that govern the motion of a fluid in any fluid flow will be presented.

Please cite this article as: Jaimes R., Nunhez J.R., 2015, Obtaining the nusselt equation with the use of cfd for a stirred tank heated with helical coils, Chemical Engineering Transactions, 43, 1687-1692 DOI: 10.3303/CET1543282

Mass conservation

$$\frac{\partial \rho}{\partial t}+\rho\left[\frac{\partial v_i}{\partial x_i}+\frac{\partial v_j}{\partial x_j}+\frac{\partial v_k}{\partial x_k}\right]=0 \quad (1)$$

Momentum conservation

$$\rho\left[\frac{\partial v_i}{\partial t}+\frac{\partial (v_i \cdot v_j)}{\partial x_j}\right]=\frac{-\partial p}{\partial x_i}+\frac{\partial}{\partial x_j}\left[\mu\left(\frac{\partial v_i}{\partial x_j}+\frac{\partial v_j}{\partial x_i}-\frac{2}{3}\delta_{ij}\,\nabla\cdot v\right)\right]+\rho g_i+\sum F_i \quad (2)$$

Energy conservation

$$\frac{\partial(\rho E)}{\partial t}+\frac{\partial\left[v_i(\rho E+p)\right]}{\partial x_i}=\frac{\partial}{\partial x_i}\left[k_{ef}\frac{\partial T}{\partial x_i}-\sum_{j'} h_{j'} J_{j',i}+v_j(\tau_{ij})_{ef}\right]+S_{ji} \quad (3)$$

Where $\rho$ is the density, $v$ is the velocity vector, $\mu$ is the effective viscosity, $p$ is the pressure, $g$ is the gravitational acceleration, $F$ is the source term, $E$ is the energy, $T$ is the temperature, $h$ is the enthalpy, $\tau$ is the viscous work term, and $S_{ji}$ is the source term, which can be considered heat sources due to chemical reactions, radiation and others. The turbulence model SST (Shear Stress Transport) was chosen due to its mixed approach between models k-ω and k-ε, which is generally known to give good results in estimating variables of interest both near to and away from the wall.

### 2.1 Stirred tank configuration

The stirred tank reactor used in this study was a standard configuration cylindrical tank with four equally spaced baffles located perpendicular to the tank wall and a set of helical coils distributed along its length. Agitation is provided by a standard six-bladed Rushton turbine impeller, as shown in Figure 1. The sizing of stirred tank with helical coils was based on the dimensions of the equipment used in the experimental work by Oldshue and Gretton (1954). Table 1 shows the geometrical dimensions used in all cases studied. The numerical experiments were conducted at impeller rotational speeds of 200, 250, 300, 350, and 500 rpm, corresponding at a Reynolds number between 5.5X10$^5$ to 1.1X10$^6$. Water at 25 °C (density = 997 kg/m$^3$, dynamic viscosity = 0.00089 kg/ms) was used as the study fluid.

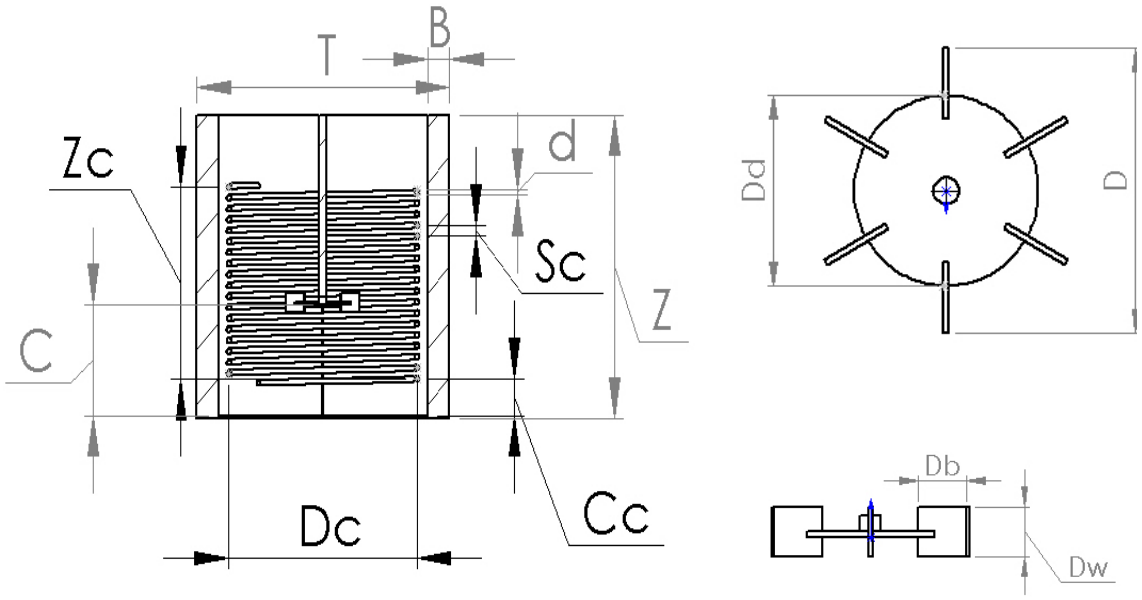


*Figure 1: Experimental geometry used by Oldshue and Gretton (1954)*

*Table 1: Tank dimensions simulated used in the simulations*

| Dimension | Symbol | Value (m) |
|---|---|---|
| Tank | T | 1.22 |
| Liquid depth | Z | 1.22 |
| Baffles width | B | 0.10 |
| Impeller height | C | 0.41 |
| Impeller diameter | D | 0.41 |
| Impeller disk thickness | s | 0.01 |
| Blade length | $D_b$ | 0.10 |
| Blade height | $D_w$ | 0.08 |
| Helix diameter | $D_c$ | 0.87 |
| Tube diameter | d | 0.04 |
| Separation between tubes | $S_c$ | 0.09 |

### 2.2 Computational method

The geometry was created using the CAD tool (DesignModeler) available by software ANSYS CFX 14.0. The symmetry of the system allowed for a reduction of the computational cost by modelling only half of the reactor. The model was further split into two regions. The internal rotating region consists of the fluid domain around three blades (i.e., half) of the impeller. The external stationary region is constituted by the tank walls, coils, and two of the baffles. A mesh was created to discretize the domain into small control volumes, where the conservation equations are approximated by algebraic equations. To create this mesh, the ANSYS CFX meshing software was used. Figure 2 shows the three-dimensional unstructured mesh with tetrahedral and prismatic elements in the rotating and stationary domains, as described above.

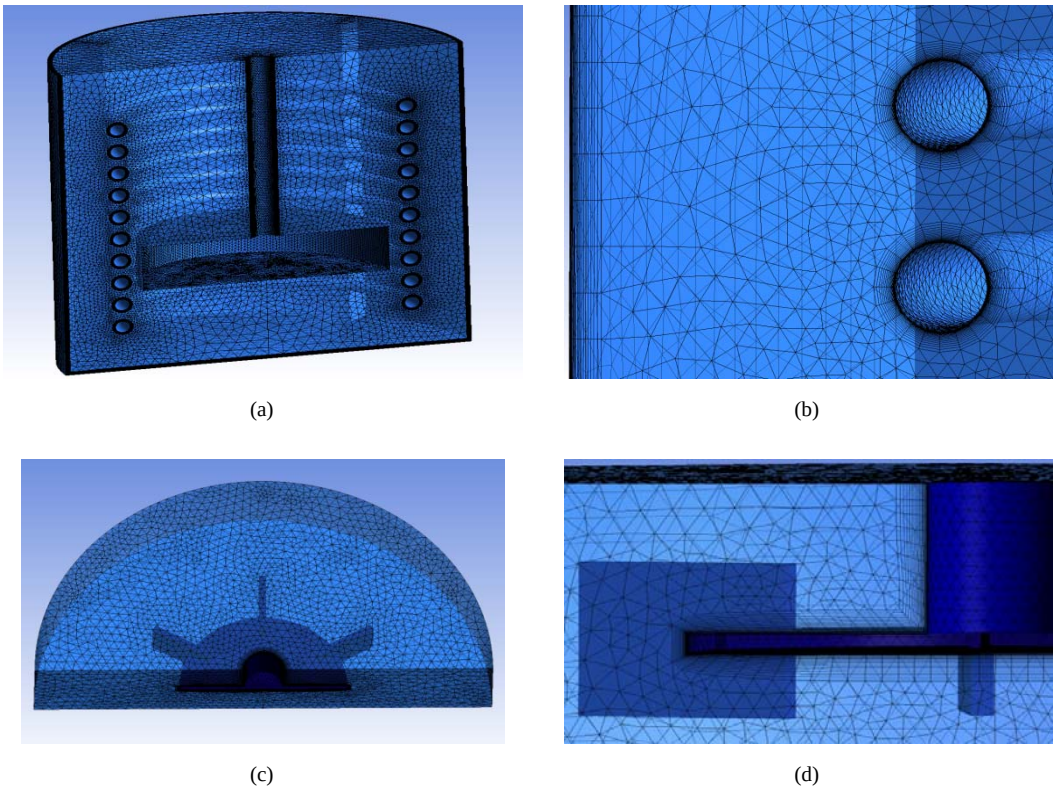

(a) (b)

(c) (d)

*Figure 2: 3D unstructured mesh with tetrahedral and prismatic elements. (a-b) Mesh surface of the stationary domain. (c-d) Surface mesh of the rotating domain*

To account for the viscous flow region near the solid surfaces such as tank walls, baffles, coils, impeller, and shaft, prismatic elements were applied. In order to ensure good results in the calculation of the fluid flow near the wall surface by the turbulence model, a dimensionless distance between 0.1 < $y^+$ <1 was used, with 20 prisms within the boundary layer (Spogis and Nunhez, 2009; Murthy and Joshi, 2008; Lane et al., 2000). The mesh contains 370,000 elements in the rotating domain and 4,500,000 in the stationary domain. Grid sensitivity studies have been conducted through the creation of different mesh densities until the numerical results showed independence from the discretization.
The following boundary conditions and assumptions were adopted for the simulations in stationary regime. The condition of non-slip was used on all solid walls (walls, bottom, baffles, impeller, shaft, and coils), so the fluid velocity is reduced in the regions close to the wall until the fluid in contact reaches zero speed at the wall. In the free surface of the liquid, the shear stresses and axial velocity are zero and a flat surface was assumed. Therefore, the free slip surface condition on the upper surface of the tank has been applied. In the both impeller and shaft was assumed that the flow velocity on the wall assumes the same angular speed defined by the rotation of impeller. Since only half of the tank geometry was simulated, cyclic boundary conditions also need to be applied. In the tubes of the serpentine has been assumed that there is enough cold liquid entering the coils to maintain a constant wall temperature of 5 ° C. When the temperature in the wall is fixed, the overall heat transfer coefficient $h_f$ is calculated as:

$$q = h_f\left(T_w - T_f\right) \tag{4}$$

Where $q$ is the wall heat flux, $T_w$ is the temperature in the wall of the coil, and $T_f$ is an average temperature of fluid. The impeller rotation was modelled using the Multiple Reference Frame (MRF) impeller model to predict the flow in the stationary regime. In all cases were considering RMS residuals values less than $1X10^{-5}$ to ensure convergence of the results (Zhang et al., 2013).

## 3. Results and discussion

Figure 3 (a) shows a comparison between the coefficient of heat transfer (Nusselt number) generated by the simulation results (Equation 4) and the heat transfer coefficient obtained in the experimental work by Oldshue Gretton (1954). The Nusselt number calculated in the CFD model presented good agreement with the experimental data for the five rotational speeds simulated; this agreement also serves as a validation of the CFD model. Figure 3 (b) shows the effect of the impeller speed (Reynolds number) on heat transfer (Nusselt number) in the conditions presented in Table 1.

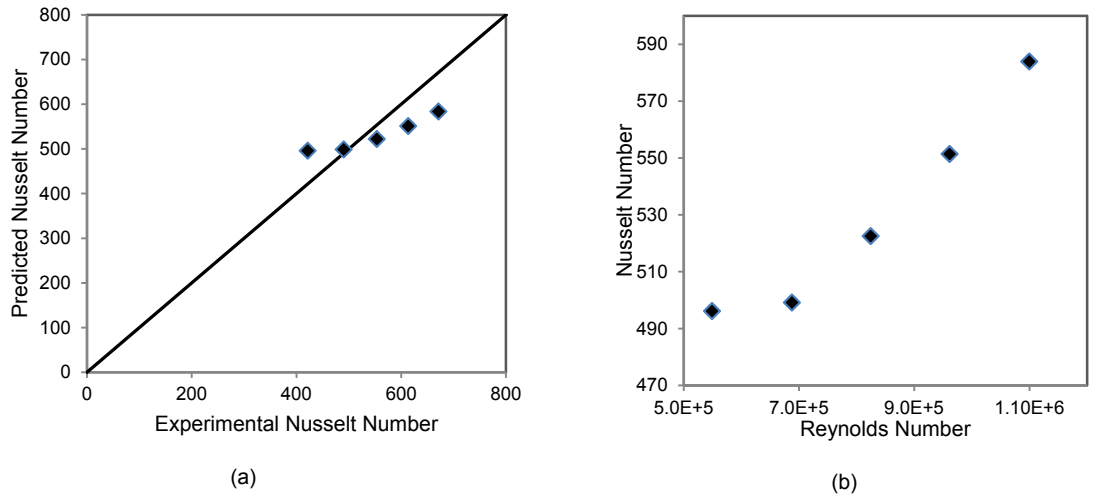


*Figure 3: (a) Comparison of experimental Nusselt number and Nusselt number calculated by CFD model. (b) Effect of rotational speed on the heat transfer for this system*

From Figure 3 (b), it can be seen that the coefficient of heat transfer increases with increasing rotational speed of the impeller. This occurs because the faster impeller creates stronger turbulence, resulting in thinner

boundary layers on the coils and therefore more effective heat exchange in the system. Figure 4 shows mean velocity vectors for radial and axial planes. In the Figure 4 (c), it can be seen that rotation of the impeller produces an intense flux in the radial direction which, when hitting the wall, divides region into two distinct recirculation zones above and below the impeller, which is typical for this type of impeller. Moreover, it can be seen in Figure 4 (a) that fluid average velocity decreases when fluid hits the coil, causing poor fluid circulation. Figure 4 (b) shows that the coils placed at the impeller blade height generate recirculation zones located between the coil and the impeller. As a consequence, there is a tendency for fluid to stagnate between the coils and the wall of the tank, as show in Figure 4 (c). Figure 4 (d) shows that in the elimination of part of the helical coil improve the flow in the regions away from the impeller and between the coil and the tank wall. This is because the velocities are higher in the proposed geometry in comparison with experimental arrangement for the same rotational speed of the impeller.

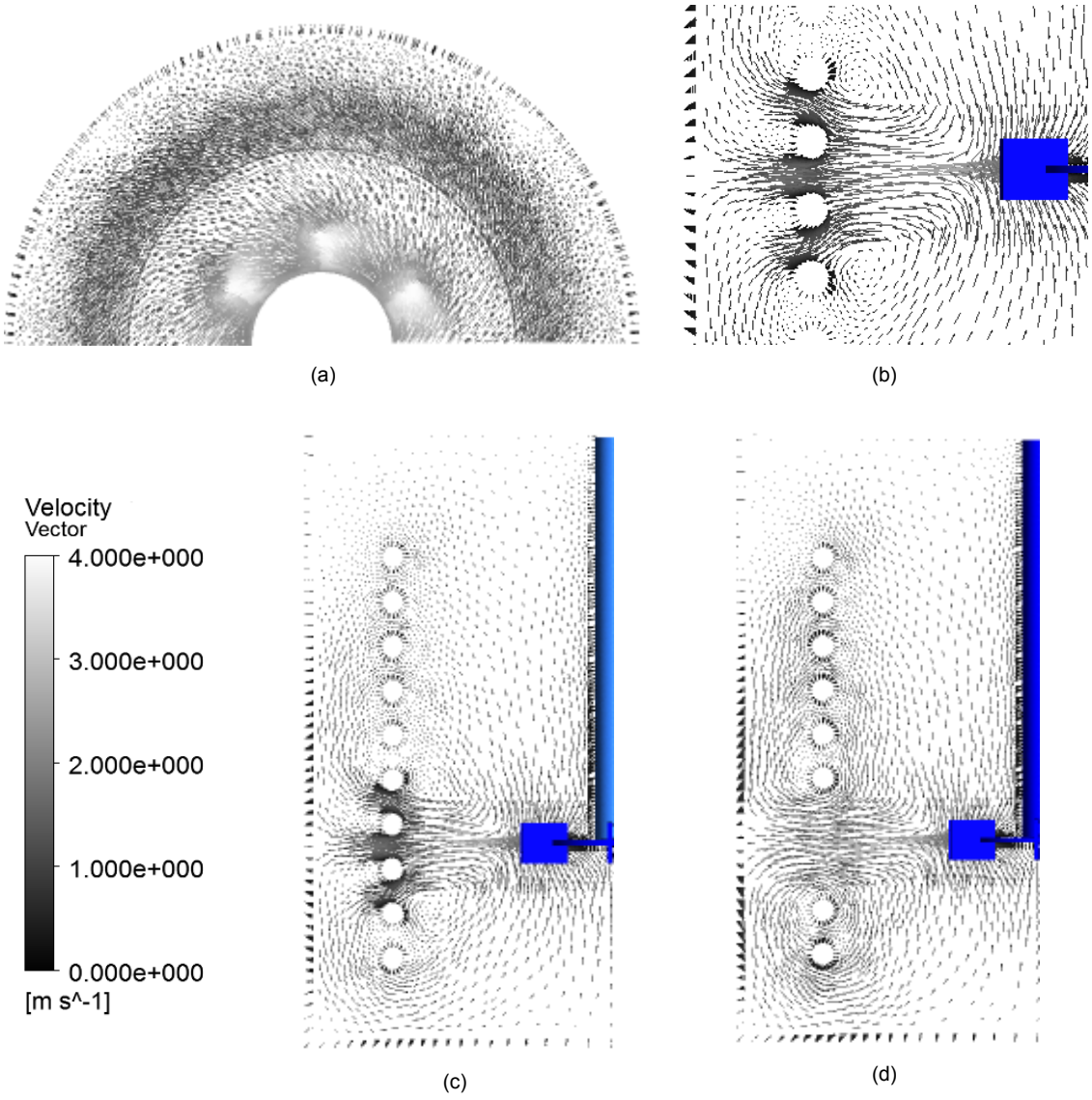


*Figure 4: Flow patterns axial and radial planes at a Reynolds number of 5.5X10$^5$. (a) Mean velocity vectors in height of impeller. (b) Mean velocity vectors near the impeller for the experimental geometry. (c) Mean velocity vectors for the Oldshue and Gretton geometry. (d) Mean velocity vectors for the Pedrosa and Nunhez geometry*

In order to see the effect of the flow patterns in the heat transfer, alternate coils were used for heating (constant flux = 160,000 W/m$^2$) and cooling (constant temperature = 5 °C) with adiabatic tank wall, similar to

what was used in the experimental work. The local heat transfer flux over the various parts of the coil is shown in Figure 5 for the two arrangements. As would be expected in Figure 5 (a), the heat transfer is better for coils near the impeller, where the flow over the surface of the coil is highest. Coils farther from the impeller experienced lower heat flux because of the reduced flow in this region. In the Figure 5 (b), it can be seen that removing the rings located at the same height of impeller improves the overall circulation of the fluid, therefore resulting in a more uniform prediction of local heat transfer across the coils.

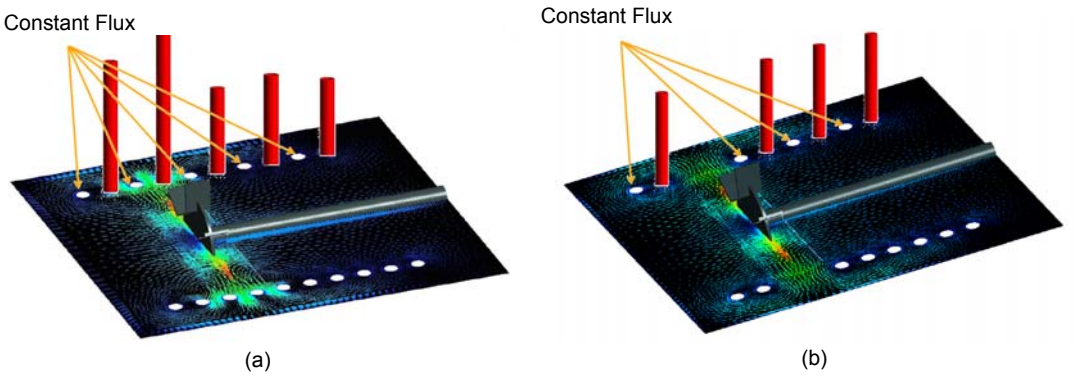


*Figure 5: Heat flow distribution at a Reynolds number of 5.5X10$^5$. (a) Heat flow distribution for the Oldshue and Gretton geometry. (b) Heat flow distribution for* the *Pedrosa and Nunhez geometry*

## 4. Conclusion

The heat transfer predictions of the CFD model have been compared with the Olshue and Gretton (1954) experimental data for five rotational speeds. The Nusselt number obtained in the model was compared with the values predicted by the experimental correlation, showing a maximum variation of 15 %. The three-dimensional model presented in this work showed good qualitative as well as quantitative agreement in terms of obtaining the Nusselt number and the flow field characteristic of the six-blade Rushton radial impeller. The effect of stirring speed on the heat transfer coefficient was also studied. As expected, the convective heat transfer coefficient increases with the increase of the impeller speed. The proposed geometry without coils placed at the same height as the impeller blades, provides better fluid circulation in the regions away from the impeller and between the coils and the wall. As a consequence, the heat flow distribution in the proposed geometry is more uniform, providing a higher overall heat transfer coefficient inside the stirred tank reactor.

**Acknowledgements**

Financial support was provided by the CAPES (*Coordenação de Aperfeiçoamento de Pessoal de Nível Superior*) and Laboratory of Computational Fluid Dynamics (LCFD) at the University of Campinas.

**References**

Lane G., Schwarz M., Evans G., Eds., 2009, Comparison of CFD Methods for Modelling of Stirred Tanks. Elsevier Science, Amsterdam, the Netherlands.

Murthy B., Joshi J., 2008, Assessment of Standard, RSM and LES Turbulence Models in a Baffled Stirred Vessel Agitated by Various Impeller Designs, Chem. Eng. Sci. 63, 5468-5495.

Oldshue J., Gretton A., 1954, Helical Coil Heat Transfer in Mixing Vessels, Chem. Eng. Prog. 50, 615-621.

Paul E., Atiemo-Obeng V., Kresta S., Eds., 2004, Handbook of Industrial Mixing: Science and Practice. Wiley-Interscience, São Paulo, Brazil.

Pedrosa S., Nunhez J., 2003, Improving Heat Transfer in Stirred Tanks Cooled by Helical Coils, Brazilian J. Chem. Eng. 20(2), 111-120.

Zhang S., Müller D., Arellano-Garcia H., Wozny G., 2013, CFD Simulation of the Fluid Hydrodynamics in a Continuous Stirred-Tank Reactor, Chemical Engineering Transactions, 32, 1441-1446, DOI: 10.3303/CET1332241

Spogis N., Nunhez J., 2009, Design of a High-Efficiency Hydrofoil Through the Use of Computational Fluid Dynamics and Multi Objective Optimization, AIChE J. 55(7), 1723-1735.